

2013


Geometry Effects on Multipole Components and Beam Optics in High-Velocity Multi-Spoke Cavities

C. S. Hopper
Old Dominion University

K. Deitrick
Old Dominion University

J. R. Delayen
Old Dominion University

Follow this and additional works at: https://digitalcommons.odu.edu/physics_fac_pubs

 Part of the [Engineering Physics Commons](#), and the [Plasma and Beam Physics Commons](#)

Repository Citation

Hopper, C. S.; Deitrick, K.; and Delayen, J. R., "Geometry Effects on Multipole Components and Beam Optics in High-Velocity Multi-Spoke Cavities" (2013). *Physics Faculty Publications*. 294.
https://digitalcommons.odu.edu/physics_fac_pubs/294

Original Publication Citation

Hopper, C. S., Deitrick, K. E., & Delayen, J. R. (2013). *Geometry effects on multipole components and beam optics in high-velocity multi-spoke cavities*. Paper presented at the North American Particle Accelerator Conference, Pasadena, California.

GEOMETRY EFFECTS ON MULTIPOLE COMPONENTS AND BEAM OPTICS IN HIGH-VELOCITY MULTI-SPOKE CAVITIES*

C. S. Hopper[†], K. Deitrick, and J. R. Delayen

Center for Accelerator Science, Department of Physics,
Old Dominion University, Norfolk, VA, 23529, USA and

Thomas Jefferson National Accelerator Facility, Newport News, VA 23606, USA

Abstract

Velocity-of-light, multi-spoke cavities are being proposed to accelerate electrons in a compact light-source [1]. There are strict requirements on the beam quality which require that the linac have only small non-uniformities in the accelerating field. Beam dynamics simulations have uncovered varying levels of focusing and defocusing in the proposed cavities, which are dependent on the geometry of the spoke in the vicinity of the beam path. Here we present the results for the influence different spoke geometries have on the multipole components of the accelerating field and how these components, in turn, impact the simulated beam properties.

INTRODUCTION

To address the varying levels of focusing and defocusing that beam dynamics simulations have shown exist, we first evaluate the higher order multipole components contained in the accelerating field to better understand what contributions could lead to the observed behavior. The design of the cavities, and the linac, are then evaluated using results generated by ASTRA particle tracking simulation code.

MULTIPOLE COMPONENTS

The higher order multipole components are analyzed using the method given in [2, 3]. Various cavities have been considered for fabrication, and the field non-uniformity for each of these cavities is shown in Fig. 2. The difference in the models essentially comes down to the shape of the spoke aperture region. A standard racetrack is preferred because of the rf properties, but a rounded square, ring [4], and elliptical aperture have also been studied, and are shown in Fig. 1.

These geometries have varying degrees of symmetry. The ring and racetrack apertures, for similar cavities, have been studied and presented elsewhere [3]. Additional optimization of apertures (c) and (d) is necessary. However, it is likely that some compromise would have to be made, in terms of increased peak surface fields, to decrease the multipole components. Figures 3 and 4 show the $E_z^{(2)}$ and $E_z^{(4)}$ components as a function of position. All the cavities have the same mesh, and similar $E_z^{(2)}$ components, however there is a clear difference in the $E_z^{(4)}$ components.

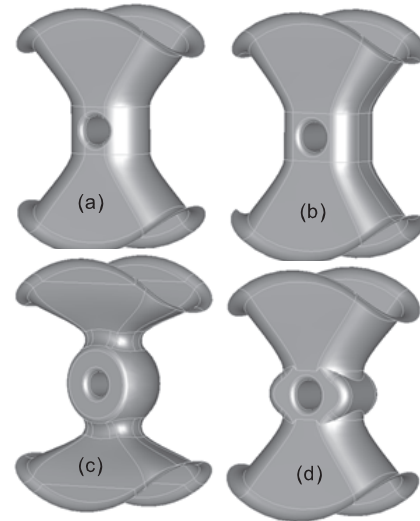


Figure 1: Various spoke aperture geometries studied. (a) racetrack, (b) rounded square, (c) ring, and (d) elliptical.

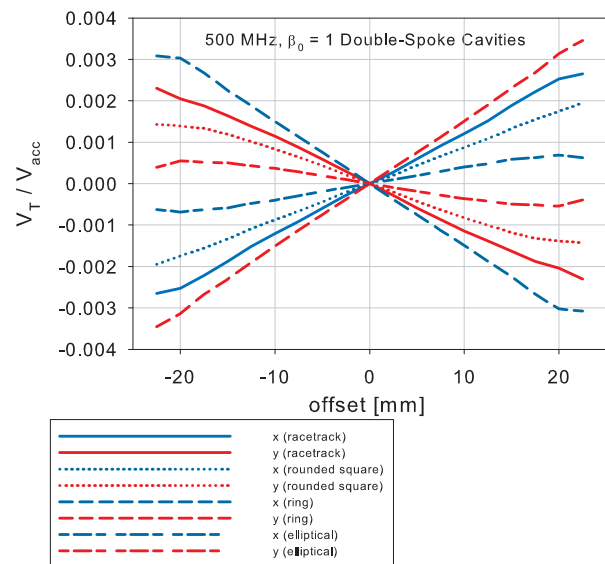
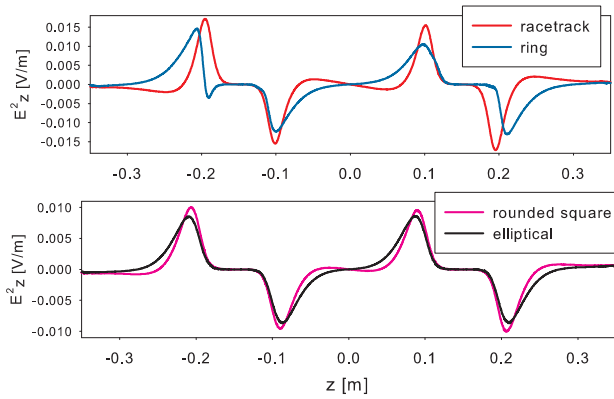
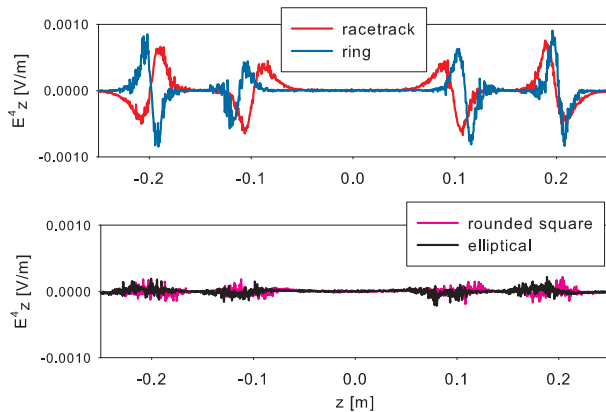


Figure 2: Dependence of transverse voltage (normalized to V_{acc}) on transverse offset for the aperture geometries presented in Fig. 1.

* Work supported by U.S. DOE Award No. DE-SC0004094

[†] chop002@odu.edu


 Figure 3: $E_z^{(2)}$ for various aperture geometries.

 Figure 4: $E_z^{(4)}$ for various aperture geometries.

With the square and elliptical aperture, the octupole component is small enough to be obscured by noise.

While there are some similarities with the studies done by [4] and [5] on HWRs and single-spoke cavities, the geometry of the spokes presented here (other than the actual aperture region) is vastly different, which makes a direct comparison difficult.

BEAM DYNAMICS

The beam dynamics were simulated using the current cathode and gun specifications, detailed in [1]. After exiting the gun, the electron beam is defocusing in both transverse directions equally. The beam then gains 5.86 MeV in the initial double-spoke cavity. The optical parameters of the beam after a single cavity are presented in Tab. 2. As the

 Table 1: Multipole Components, 500 MHz, $\beta_0 = 1$

Aperture Geometry	\mathbf{b}_2 [mT]	\mathbf{b}_4 [mT/m ²]
Racetrack	$0.37 + 0.006i$	$-3.9 + 720i$
Rounded Square	$0.25 - 0.001i$	N/A
Ring	$-0.45 - 0.07i$	$141 - 264i$
Elliptical	$-0.1 - 0.001i$	N/A

spoke cavities are not symmetric with respect to the beam line, the transverse components are no longer equal, which is expected. However, the difference between the transverse components of either α or β differs between the four designs. With the least difference is the elliptical aperture, while the ring aperture has the most. Another noteworthy point is that after a single cavity, the β_x and β_y of the beam are diverging for the designs that are not the elliptical aperture.

At the exit of the cavity, a perfectly round beam would be such that $\beta_x = \beta_y$. After passing through a single cavity, the list of apertures in order of decreasing roundness is as follows: elliptical, rounded square, racetrack, and ring. This is also the order that would be obtained by listing apertures in order of increasing $|b_2|$. A comparison of the beam spots for the four designs with optimal configuration after one cavity is seen in Fig. 5.

The results become even more interesting when the electron beam passes through two cavities, shown in Tab. 3. The (-) entries correspond to an iris-to-iris distance of 0.619 m separating the two cavities, while (S) corresponds to a distance of 0.255 m. Entries with (R) correspond to the second cavity rotated 90° as in [1], so that the first spoke in the second cavity the beam traverses is orthogonal to the first spoke in the first cavity that the beam passes through. A few conclusions can be formed. Both the ring and elliptical apertures have β_x and β_y diverging, regardless of the separation or orientation of the second cavity. The racetrack and rounded square apertures diverge for either separation if the second cavity is unrotated, while the β_x and β_y converge for either separation if the second cavity is rotated.

More narrow observations can be made. For both distances, a rotated second cavity produces a rounder beam except for the (-) elliptical. Given that this technique works on the elliptical if there is a shorter separation distance, it may be that if a beam is round to the first order at the exit of an unrotated second cavity, rotating the second cavity decreases the roundness of the resulting beam. The beam behavior similar to a quadrupole is when the beam focuses in one direction while defocusing in the other, which corresponds to each transverse component of α having a different sign.

Since it has now become clear that the separation between the two cavities does have an impact that differs between designs, it is difficult to form any firm conclusions. It is possible to configure the racetrack and rounded square cavities to produce a converging beam for two cavities, while it is impossible to do so with the ring and elliptical designs, regardless of the distance between the two cavities. To develop further conclusions would require a systematic sweep over different separation distances and orientation of the second cavity for all four aperture designs. Though a worthwhile topic, it is beyond the scope of this paper.

As the quadrupole moment is significant in all four of the presented designs, it is difficult to discern the impact of

Table 2: Beam Properties After a Single Cavity

Aperture Geometry	α_x	α_y	β_x [m]	β_y [m]
Racetrack	-19.58	-12.34	55.31	45.67
Rounded Square	-20.21	-16.34	55.51	49.46
Ring	-4.687	-26.27	44.38	56.87
Elliptical	-16.90	-18.47	53.42	51.28

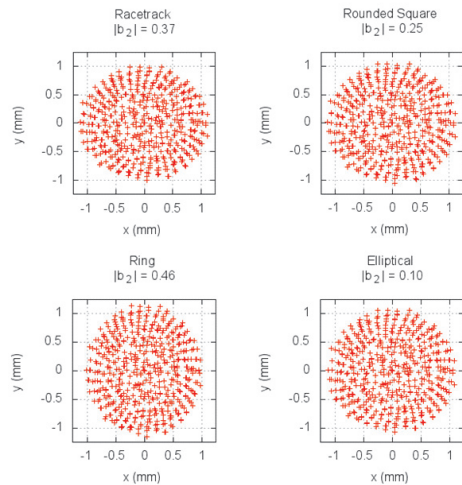


Figure 5: Beam spots of the different designs, with corresponding $|b_2|$ values, after a single cavity.

the octupole moment on the beam. Consequently, we are unable to form any conclusions about the relationship between $|b_4|$ and the behavior of the beam. A study of this aspect would require the quadrupole moment of the compared designs to be sufficiently constant. Additionally, it would also require a reliable method of accurately integrating $E_z^{(4)}$, which is difficult for the rounded square and elliptical apertures, as seen in Fig. 4.

To emphasize the connection between the beam behavior and $|b_2|$ for a given aperture design, this analysis begins with a single cavity. Once a second is added and it becomes clear that the separation between the two also has an impact, making it difficult to discern the consequences of separation and $|b_2|$ from the current set of results. Given a linac consisting of four cavities, separated as in [1], the optimum results are shown in Tab. 4. Optimal configurations for all designs except the elliptical are obtained by rotating the second and fourth cavity. For the elliptical, the optimum results are obtained by rotating only the third cavity.

CONCLUSION

The multipole components and beam optics have been studied for different spoke aperture geometries. A racetrack shaped aperture provides the most desirable rf properties, and with the proper orientation, an acceptable beam shape. The fabrication of this cavity is underway at Jefferson Lab.

Table 3: Beam Properties after Two Cavities, with the Second Cavity Rotated (R), Closer to the First Cavity (S), or Both (RS)

Aperture Geometry	α_x	α_y	β_x [m]	β_y [m]
Racetrack (-)	-15.6	0.234	106	65.1
Rounded Square (-)	-15.3	-5.13	107	81.6
Ring (-)	7.15	-27.5	45.2	128
Elliptical (-)	-8.98	-8.85	93.1	91.0
Racetrack (-R)	-4.40	-7.74	92.6	75.6
Rounded Square (-R)	-7.90	-11.4	97.1	90.4
Ring (-R)	-0.069	-8.45	49.2	118
Elliptical (-R)	-6.34	-11.6	87.3	97.2
Racetrack (S)	-13.8	-0.202	86.0	55.5
Rounded Square (S)	-13.6	-5.12	86.3	67.2
Ring (S)	6.95	-24.9	43.1	102
Elliptical (S)	6.13	-27.9	46.8	109
Racetrack (RS)	-4.98	-6.95	76.2	64.0
Rounded Square (RS)	-7.86	-10.3	79.0	74.2
Ring (RS)	0.148	-10.1	46.0	94.8
Elliptical (RS)	-1.22	-12.0	49.9	101

Table 4: Beam Properties After Four Cavities, Configured to Produce Roundest Beam

Aperture Geometry	α_x	α_y	β_x [m]	β_y [m]
Racetrack	5.555	2.035	94.68	78.64
Rounded Square	2.896	-0.1997	109.9	106.8
Ring	4.782	4.879	31.46	132.9
Elliptical	1.945	1.567	103.5	108.5

REFERENCES

- [1] T. Satogata et al, "Compact Accelerator Design for a Compton Light Source," IPAC 2013, Shanghai, China, May 2013.
- [2] J. Barranco Garcia et al, "Study of Multipolar RF Kicks from the Main Deflecting Mode in Compact Crab Cavities for LHC" IPAC 2012, New Orleans, LA, (2012), p. 1873.
- [3] R. G. Olave, J. R. Delayen, and C. S. Hopper, "Multipole Expansion of the Fields in Superconducting High-Velocity Spoke Cavities," LINAC 2012, Tel Aviv, Israel, September 2012.
- [4] B. Mustapha, P.N. Ostroumov and Z.A. Conway, "A Ring-Shaped Center Conductor Geometry for a Half-Wave Resonator," IPAC 2012, New Orleans, LA, (2012), WEPPC037.
- [5] P. Berrutti et al, "Effects of RF Field Asymmetry in SC Cavities of the Project X," IPAC 2012, New Orleans, LA, (2012), pp. 2318-2320.